



Secondary bonding in dimethylbis(morpholine-4-carbodithioato- κ^2S,S')tin(IV): crystal structure and Hirshfeld surface analysis

Nordiyana Binti Zaldi,^a Rusnah Syahila Duali Hussien,^a See Mun Lee,^b Nathan R. Halcovitch,^c Mukesh M. Jotani^{d‡} and Edward R. T. Tiekink^{e*}

Received 4 May 2017

Accepted 7 May 2017

Edited by W. T. A. Harrison, University of Aberdeen, Scotland

‡ Additional correspondence author, e-mail: mmjotani@rediffmail.com.

Keywords: crystal structure; organotin; dithiocarbamate; tetrel bonding; Hirshfeld surface analysis.

CCDC reference: 1548414

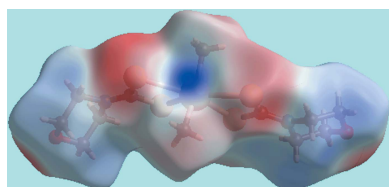
Supporting information: this article has supporting information at journals.iucr.org/e

^aDepartment of Chemistry, University of Malaya, 50603 Kuala Lumpur, Malaysia, ^bResearch Centre for Crystalline Materials, School of Science and Technology, Sunway University, 47500 Bandar Sunway, Selangor Darul Ehsan, Malaysia, ^cDepartment of Chemistry, Lancaster University, Lancaster LA1 4YB, United Kingdom, ^dDepartment of Physics, Bhavan's Sheth R. A. College of Science, Ahmedabad, Gujarat 380 001, India, and ^eResearch Centre for Chemical Crystallography, School of Science and Technology, Sunway University, 47500 Bandar Sunway, Selangor Darul Ehsan, Malaysia. *Correspondence e-mail: edwardt@sunway.edu.my

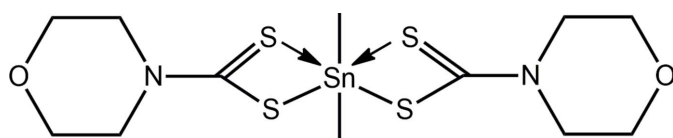
The title compound, [Sn(CH₃)₂(C₅H₈NOS₂)₂], has the Sn^{IV} atom bound by two methyl groups which lie over the weaker Sn–S bonds formed by two asymmetrically chelating dithiocarbamate ligands so that the coordination geometry is skew-trapezoidal bipyramidal. The most prominent feature of the molecular packing are secondary Sn···S interactions [Sn···S = 3.5654 (7) Å] that lead to centrosymmetric dimers. These are connected into a three-dimensional architecture *via* methylene-C–H···S and methyl-C–H···O(morpholino) interactions. The Sn···S interactions are clearly evident in the Hirshfeld surface analysis of the title compound along with a number of other intermolecular contacts.

1. Chemical context

Both binary tin and organotin dithiocarbamates, R_nSn(S₂CNRR')_m for n + m = 4, are well known to exhibit potential biological properties, *e.g.* anti-cancer (Ferreira *et al.*, 2014), anti-fungal (Yu *et al.*, 2014) and anti-microbial (Ferreira *et al.*, 2012), as well to serve as useful molecular precursors for the generation of 'SnS' nanomaterials (Kevin *et al.*, 2015). The structural chemistry of this class of compound has also attracted considerable interest over the years owing to the occurrence of significant structural diversity observed in seemingly closely related compounds (Tiekink, 2008). As a case in point and related to the title compound, [Sn(CH₃)₂(C₅H₈NOS₂)₂] (I), reported herein, are the variations in molecular structure observed for the diorganotin bis(dithiocarbamate)s as discussed in the recent literature (Muthalib *et al.*, 2014; Mohamad *et al.*, 2016, 2017). These R₂Sn(S₂CNRR')₂ structures are known to adopt four distinct coordination geometries with the majority being skew-trapezoidal bipyramidal or octahedral, each based on C₂S₄ donor sets. Fewer examples are known for five-coordinate, trigonal-bipyramidal species, *e.g.* (t-Bu)₂Sn(S₂CNMe₂)₂ in which one dithiocarbamate ligand is monodentate (Kim *et al.*, 1987), and seven-coordinate, pentagonal-bipyramidal, *e.g.* [MeOC(=O)CH₂CH₂]₂Sn(S₂CNMe)₂ where the carbonyl-O atom of one Sn-bound organic substituent is also coordinating the tin atom (Ng *et al.*, 1989). This last example is of interest as



it demonstrates tin may in fact increase its coordination number by additional interactions. When additional interactions of this type occur intermolecularly, they are termed secondary bonding or tetrel bonding as a Group IV element, tin, is involved (Alcock, 1972; Marín-Luna *et al.*, 2016; Tiekink, 2017). Generally, secondary interactions do not occur for $R_2\text{Sn}(\text{S}_2\text{CNRR}')_2$ structures as the strong chelating ability of the dithiocarbamate ligand reduces the Lewis acidity of the tin atom. However, in (I) such secondary $\text{Sn} \cdots \text{S}$ interactions do in fact occur. In a continuation of work in this area, herein the synthesis and crystal and molecular structures of (I) are described as well as an analysis of the Hirshfeld surface with a particular emphasis on investigating the role of the secondary $\text{Sn} \cdots \text{S}$ interaction.



2. Structural commentary

The Sn^{IV} atom in the title compound (I), Fig. 1, adopts one of the common coordination geometries found for $R_2\text{Sn}(\text{S}_2\text{CNRR}')_2$ molecules, *i.e.* skew-trapezoidal bipyramidal rather than octahedral (Tiekink, 2008). This arises as the chelating dithiocarbamate ligands have asymmetric $\text{Sn}-\text{S}$ bond lengths, Table 1. The values of $\Delta(\text{Sn}-\text{S}) = [d(\text{Sn}-\text{S}_{\text{long}}) - d(\text{Sn}-\text{S}_{\text{short}})]$ for the S1- and S3-dithiocarbamate ligands are approximately the same at 0.35 Å, but the comparable bonds formed by the S3-dithiocarbamate ligand are systematically longer than those formed by the S1-dithiocarbamate ligand by approximately 0.02 Å, Table 1. The asymmetry in the $\text{Sn}-\text{S}$ bond lengths is reflected in the disparity in the associated $\text{C}-\text{S}$ bond lengths with the sulfur atom forming the longer $\text{Sn}-\text{S}$ bond being involved in the significantly shorter, by approximately 0.05 Å, $\text{C}-\text{S}$ bond, Table 1. Consistent with the skew-trapezoidal bipyramidal geometry about the Sn^{IV} atom, the Sn -bound methyl substituents are directed over the longer $\text{Sn}-\text{S}$ bonds and define an angle of 148.24 (11)° at the tin atom. The angle subtended at the tin atom by the strongly bound sulfur atoms of 85.878 (19)° is significantly less than

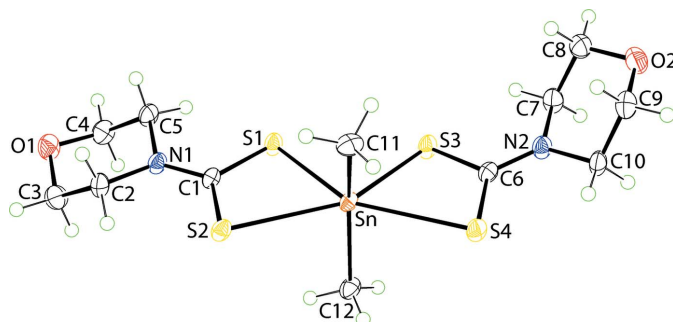


Figure 1

The molecular structure of (I), showing the atom-labelling scheme and displacement ellipsoids at the 50% probability level.

Table 1

Selected geometric parameters (Å, °).

$\text{Sn}-\text{S1}$	2.5429 (6)	$\text{Sn}-\text{C12}$	2.111 (3)
$\text{Sn}-\text{S2}$	2.8923 (6)	$\text{C1}-\text{S1}$	1.747 (3)
$\text{Sn}-\text{S3}$	2.5649 (7)	$\text{C1}-\text{S2}$	1.702 (3)
$\text{Sn}-\text{S4}$	2.9137 (6)	$\text{C6}-\text{S3}$	1.750 (3)
$\text{Sn}-\text{C11}$	2.132 (3)	$\text{C6}-\text{S4}$	1.697 (3)
$\text{S1}-\text{Sn}-\text{S2}$	65.935 (19)	$\text{S2}-\text{Sn}-\text{C12}$	84.93 (8)
$\text{S1}-\text{Sn}-\text{S3}$	85.878 (19)	$\text{S3}-\text{Sn}-\text{S4}$	65.137 (18)
$\text{S1}-\text{Sn}-\text{S4}$	150.95 (2)	$\text{S3}-\text{Sn}-\text{C12}$	102.37 (8)
$\text{S1}-\text{Sn}-\text{C11}$	99.49 (8)	$\text{S3}-\text{Sn}-\text{C11}$	99.28 (8)
$\text{S1}-\text{Sn}-\text{C12}$	104.96 (8)	$\text{S4}-\text{Sn}-\text{C11}$	84.20 (8)
$\text{S2}-\text{Sn}-\text{S3}$	151.798 (18)	$\text{S4}-\text{Sn}-\text{C12}$	84.15 (7)
$\text{S2}-\text{Sn}-\text{S4}$	143.066 (18)	$\text{C11}-\text{Sn}-\text{C12}$	148.24 (11)
$\text{S2}-\text{Sn}-\text{C11}$	86.87 (8)		

that formed by the weakly bound sulfur atoms, *i.e.* 143.066 (18)°, and is largely responsible for the formation of the skew-trapezoidal plane about the tin atom.

3. Supramolecular features

An interesting feature of the molecular packing in (I) is the formation of a supramolecular dimer sustained by $\text{Sn} \cdots \text{S}$ secondary interactions, as shown in Fig. 2*a*, where two long edges of the translationally displaced trapezoidal planes approach each other to form the interactions. Here, $\text{Sn} \cdots \text{S}^{\text{II}}$ is 3.5654 (7) Å, which is approximately 0.4 Å shorter than the sum of the van der Waals radii of Sn and S of 3.97 Å (Bondi, 1964); symmetry operation (i): $1-x, 1-y, 1-z$. Connections between the dimeric aggregates are of the type methylene- $\text{C}-\text{H} \cdots \text{S}$ and methyl- $\text{C}-\text{H} \cdots \text{O}$ (morpholino), Table 2, and these

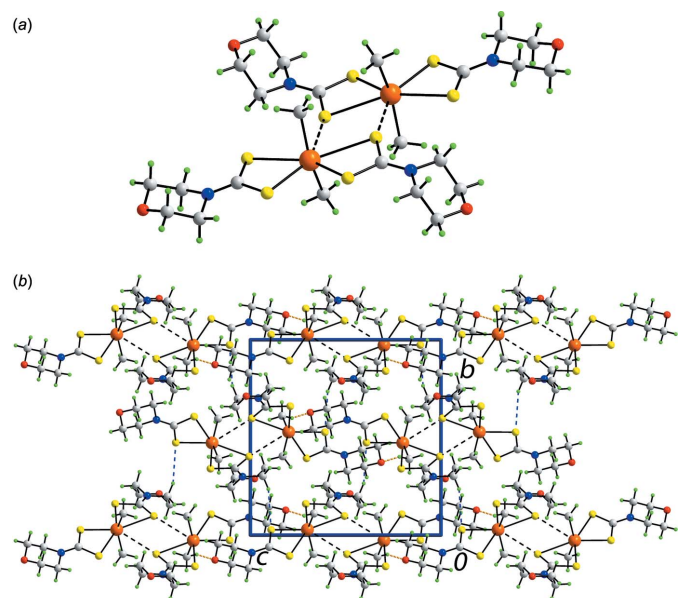


Figure 2

The molecular packing in (I), showing (a) a supramolecular dimer sustained by $\text{Sn} \cdots \text{S}$ secondary interactions shown as black dashed lines and (b) a view of the unit-cell contents in projection down the a axis. The $\text{C}-\text{H} \cdots \text{S}$ and $\text{C}-\text{H} \cdots \text{O}$ interactions are shown as orange and blue dashed lines, respectively.

Table 2
Hydrogen-bond geometry (Å, °).

$D-H\cdots A$	$D-H$	$H\cdots A$	$D\cdots A$	$D-H\cdots A$
C10—H10A \cdots S1 ⁱ	0.99	2.86	3.809 (3)	161
C12—H12C \cdots O1 ⁱⁱ	0.98	2.47	3.399 (4)	158

Symmetry codes: (i) $x - \frac{3}{2}, -y - \frac{1}{2}, z - \frac{3}{2}$; (ii) $-x + 2, -y + 1, -z + 1$.

interactions combine to generate a three-dimensional architecture, Fig. 2b.

4. Hirshfeld surface analysis

The Hirshfeld surfaces calculated on the structure of (I) also provide insight into the supramolecular association through secondary Sn \cdots S, S \cdots S and other contacts, and was performed as per recent publications on related organotin dithiocarbamate structures (Mohamad *et al.*, 2017, 2016). The broad, bright-red spots appearing near the Sn and S4 atoms on the Hirshfeld surfaces mapped over d_{norm} in Fig. 3a indicate the formation of the supramolecular dimer through secondary Sn \cdots S contacts. On the Hirshfeld surface mapped over elec-

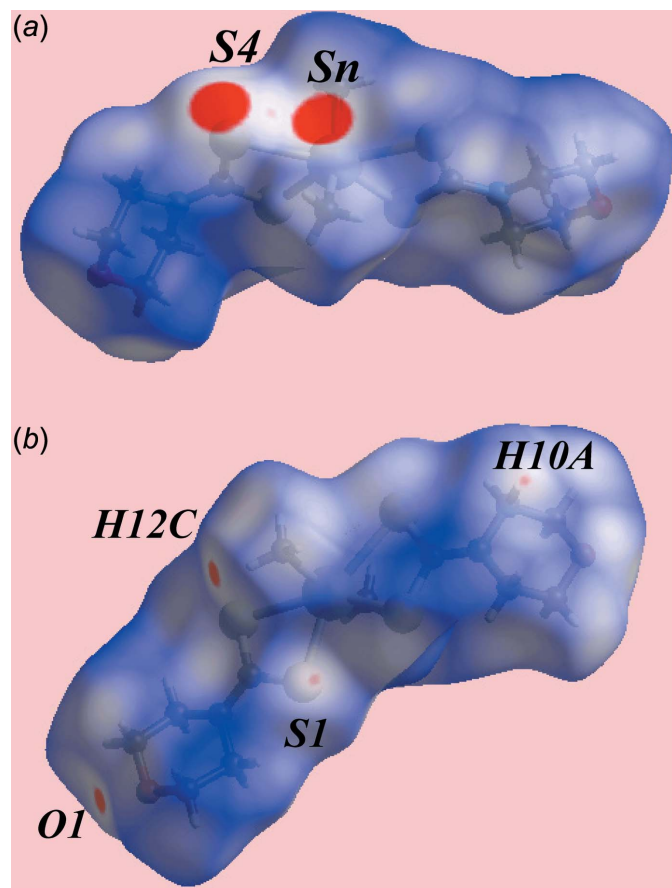


Figure 3
Two views of the Hirshfeld surface for (I) plotted over d_{norm} in the range -0.050 to 1.780 au.

Table 3
Summary of short inter-atomic contacts (Å) in (I).

Contact	distance	symmetry operation
S4 \cdots S4	3.5835 (10)	$1 - x, 1 - y, -z$
S2 \cdots H12B	2.99	$\frac{3}{2} - x, \frac{1}{2} + y, \frac{1}{2} - z$
S3 \cdots H5B	2.94	$1 - x, 1 - y, 1 - z$
S4 \cdots H11C	2.94	$1 - x, 1 - y, -z$
O2 \cdots H2A	2.63	$\frac{1}{2} - x, -\frac{1}{2} + y, \frac{1}{2} - z$
O2 \cdots H5B	2.70	$\frac{1}{2} - x, -\frac{1}{2} + y, \frac{1}{2} - z$
C1 \cdots H3A	2.88	$2 - x, 1 - y, 1 - z$
C3 \cdots H12C	2.86	$2 - x, 1 - y, 1 - z$
H2A \cdots H11C	2.36	$\frac{1}{2} + x, \frac{3}{2} - y, \frac{1}{2} + z$

trostatic potential in Fig. 4, these interactions are represented by the blue and red regions around these atoms, respectively. The faint-red spot appearing between the above bright-red spots near the S4 atom indicates the short inter-atomic S \cdots S contact, Table 3, between S4 atoms lying on diagonally opposite vertices of a parallelogram formed by symmetry-related Sn and S4 atoms, Fig. 5a. The pair of bright-red spots appearing near the methyl-H12C and morpholine-O1 atoms in Fig. 3b represent the respective donor and acceptor atoms of the C12—H \cdots O1 interaction. The comparatively weaker methylene-C10—H \cdots S1 interaction is viewed as a pair of faint-red spots near these atoms in Fig. 3b. It is important to note from the immediate environments about a reference molecule within d_{norm} -mapped Hirshfeld surfaces highlighting intermolecular interactions in Fig. 5 that the secondary Sn \cdots S and S \cdots S contacts are on one side of the Hirshfeld surface while the atoms participating in C—H \cdots O and C—H \cdots S interactions are on the other side of the surface.

The overall two-dimensional fingerprint plot, Fig. 6a, and those delineated into H \cdots H, S \cdots H/H \cdots S, O \cdots H/H \cdots O, C \cdots H/H \cdots C, N \cdots H/H \cdots N, Sn \cdots S/S \cdots Sn and S \cdots S contacts (McKinnon *et al.*, 2007) are illustrated in Fig. 6b–h, respectively; the relative contributions from the various contacts to the Hirshfeld surfaces are summarized in Table 4.

In the fingerprint plot delineated into H \cdots H contacts, Fig. 6b, the points forming the single short peak at $d_e + d_i < 2.4$ Å are indicative of the short inter-atomic H \cdots H contact listed in Table 3. The involvement of S1 in the C—H \cdots S interaction

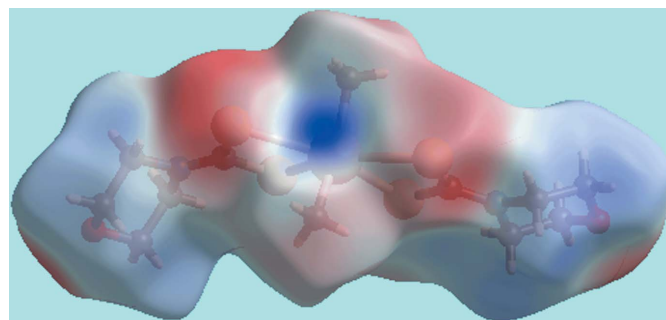


Figure 4
A view of Hirshfeld surface for (I) mapped over the calculated electrostatic potential in the range -0.053 to $+0.078$ au. The red and blue regions represent negative and positive electrostatic potentials, respectively.

Table 4
Percentage contributions of inter-atomic contacts to the Hirshfeld surfaces for (I).

Contact	percentage contribution
H...H	56.8
S...H/H...S	27.2
O...H/H...O	9.9
C...H/H...C	4.0
N...H/H...N	1.1
Sn...S/S...Sn	0.5
S...S	0.5

and other sulfur atoms in short inter-atomic S...H/H...S contacts, Table 3, results in an overall 27.2% contribution to the Hirshfeld surface. In the fingerprint plot delineated into S...H/H...S contacts, Fig. 6c, they appear as overlapping

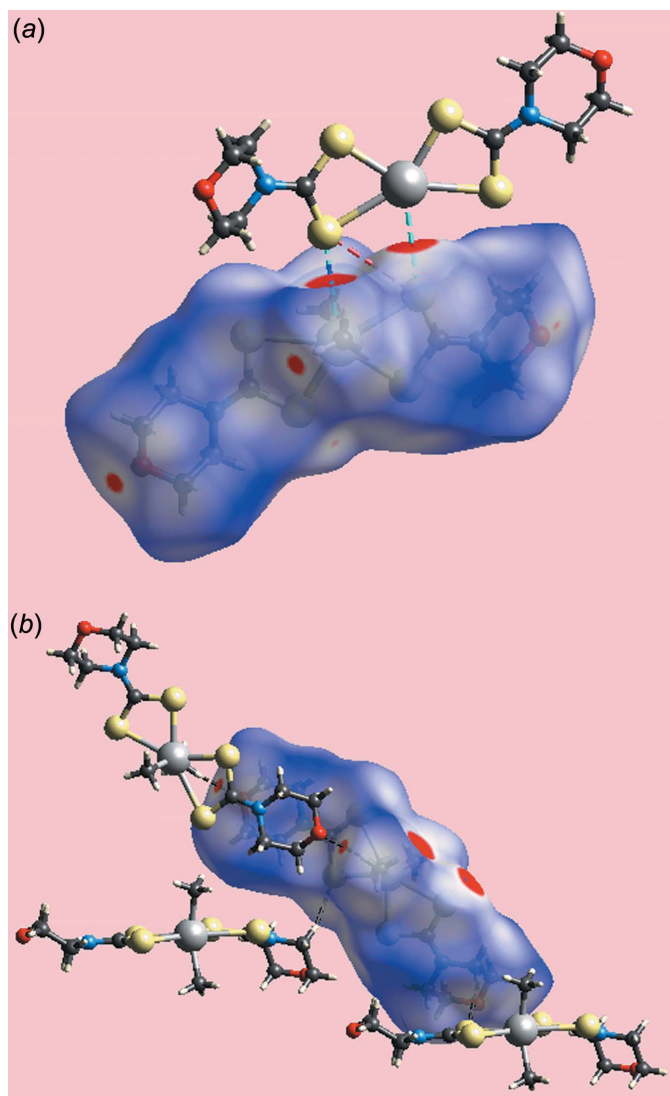


Figure 5
Views of Hirshfeld surfaces mapped over d_{norm} about a reference molecule showing (a) secondary Sn...S/S...Sn and S...S contacts by sky-blue and red dashed lines, respectively and (b) C—H...O and C—H...S interactions by black dashed lines

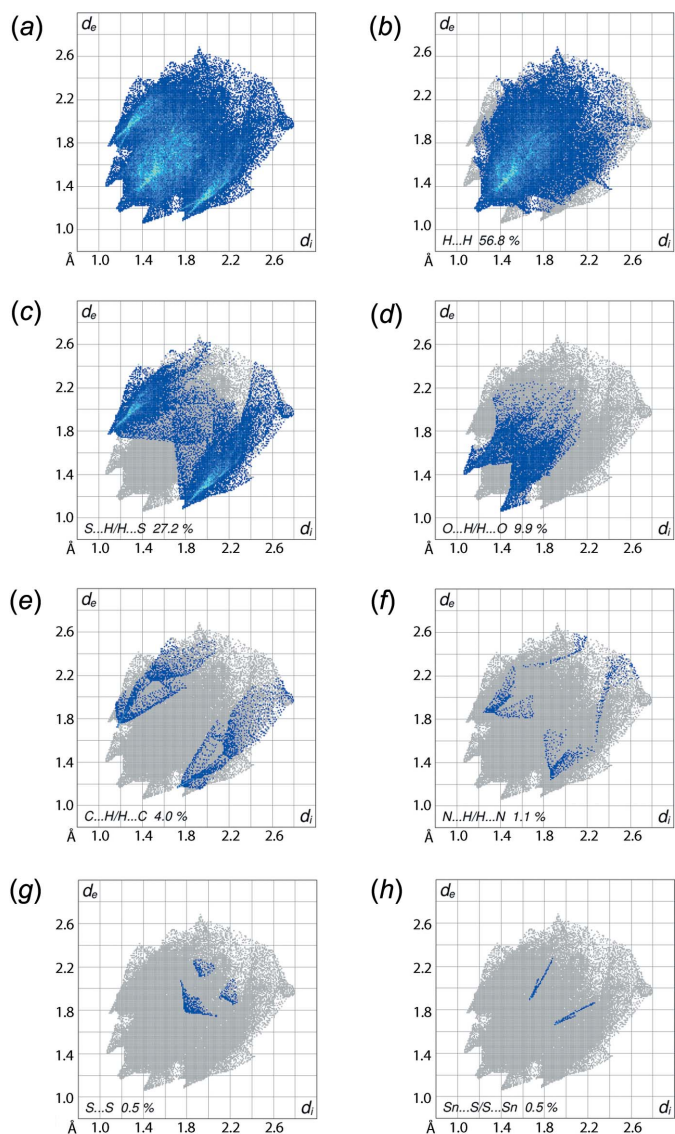


Figure 6
(a) The full two-dimensional fingerprint plot for (I) and fingerprint plots delineated into (b) H...H, (c) S...H/H...S, (d) O...H/H...O, (e) C...H/H...C, (f) N...H/H...N, (g) Sn...S/S...Sn and (h) S...S contacts.

donor–acceptor regions showing corners and a pair of greenish regions of greater intensity having short spikes at $d_e + d_i \sim 2.9$ Å. The C—H...O contact is evident from the two-dimensional fingerprint plot delineated into O...H/H...O contacts, Fig. 6d, as the pair of tips at $d_e + d_i \sim 2.5$ Å in the forceps-like distribution. The short inter-atomic O...H/H...O contacts, Table 3, in the plot appear as faint-green points in a slightly scattered form emanating from $d_e + d_i \sim 2.9$ Å. The pair of short spikes at $d_e + d_i < 2.9$ Å overlapping on the well separated donor and acceptor regions in the fingerprint plot delineated into C...H/H...C contacts, Fig. 6e, indicate the influence of short inter-atomic C...H/H...C contacts, Table 3. The presence of secondary Sn...S and short S...S contacts in the structure is also confirmed from the respective plots through the distribution of points as

Table 5
Summary of Sn—S, Sn···S distances (Å) in $R_2\text{Sn}(\text{S}_2\text{CNRR}')_2$ structures featuring secondary Sn···S interactions.

<i>R</i>	<i>R, R'</i>	Sn—S _{short} , Sn—S _{long}	Sn···S	motif	Reference
Me	Et, Et	2.5174 (18), 2.961 (3); 2.528 (2), 2.9162 (17)	3.853 (2)	<i>A</i>	Morris & Schlemper (1979)
Me	(CH ₂ CH ₂)Me	2.5367 (14), 2.9171 (16); 2.5577 (15), 2.8953 (16)	3.6978 (18)	<i>A</i>	Zia-ur-Rehman <i>et al.</i> (2007)
Me	(CH ₂ CH ₂)O	2.5429 (6), 2.8923 (6); 2.5649 (7), 2.9137 (6)	3.5654 (7)	<i>A</i>	this work
C(H)=CH ₂	Cy	2.514 (5), 2.914 (4); 2.536 (4), 2.914 (4)	3.662 (5)	<i>A</i>	Hall & Tiekink (1998)
CH ₂ Ph	Et, Et	2.5310 (11), 2.8940 (11); 2.5396 (10), 2.9109 (11)	3.8161 (12)	<i>A</i>	Yin <i>et al.</i> (2003)
CH ₂ PhCl-2	(CH ₂ CH ₂)NMe	2.5401 (13), 2.8050 (13); 2.5675 (13), 2.8675 (12)	3.9071 (13)	<i>A</i>	Yin & Xue (2005a)
CH ₂ PhCl-3 ^a	(CH ₂ CH ₂)NEt	2.520 (3), 2.840 (3); 2.556 (2), 2.893 (3)	3.638 (3)	<i>A</i>	Xue <i>et al.</i> (2005)
CH ₂ PhCl-4	(CH ₂ CH ₂)NMe	2.534 (2), 2.968 (3); 2.550 (2), 2.858 (3)	3.765 (3)	<i>A</i>	Yin & Xue (2005b)
CH ₂ PhCN-4	Et, Et	2.524 (3), 2.885 (3); 2.537 (2), 2.879 (2)	3.821 (3)	<i>A</i>	Yin & Xue (2006)
Me ^b	Et; CH ₂ Ph	2.543 (2), 2.943 (2); 2.549 (2), 2.909 (2)	3.724 (3)	<i>B</i>	Barba <i>et al.</i> (2012)
		2.579 (2), 2.842 (2); 2.609 (2), 3.003 (2)	2.978 (5) ^c		
Me ^d	CH ₂ Ph, 0.5(1,3-CH ₂ C ₆ H ₄ CH ₂)	2.5086 (13), 2.8791 (15); 2.5217 (14), 3.1510 (16)	3.9641 (15)	<i>C</i>	Santacruz-Juárez <i>et al.</i> (2008)
Me ^{d,e}	bicyclo[2.2.1]hept-2yl, 0.5(CH ₂) ₄	2.5179 (12), 2.9015 (13); 2.5321 (12), 2.9600 (13)	3.9453 (14)	<i>C</i>	Rojas-León <i>et al.</i> (2012)
Me ^f	(CH ₂) ₂ ^{Pr} , 0.5(1,3-CH ₂ C ₆ H ₄ CH ₂)	2.5319 (18), 2.8855 (18); 2.5356 (17), 2.9663 (19)	4.0480 (19)	<i>C'</i>	Santacruz-Juárez <i>et al.</i> (2008)
		2.5306 (17), 2.9492 (19); 2.5402 (19), 2.9633 (19)	3.7050 (17)		

Notes: (a) piperazine mono-solvate; (b) two molecules in the asymmetric unit; (c) Sn···N secondary interaction; (d) the binuclear molecule is located about a centre of inversion; (e) CDCl₃ di-solvate per binuclear entity; (f) two molecules in the asymmetric unit with each being located about a centre of inversion.

a pair of thin line segments, Fig. 6f, and a triangle, Fig. 6g, respectively, having minimum $d_c + d_1$ distances at around 3.5 Å and 3.6 Å, respectively. The 1.1% contribution from N···H/H···N contacts, Fig. 6h, to the Hirshfeld surface reflects an insignificant influence upon the molecular packing as the interatomic separations are greater than the sum of the respective van der Waals radii.

5. Database survey

The Cambridge Crystallographic Database (Groom *et al.*, 2016) contains over 110 molecules of the general formula $R_2\text{Sn}(\text{S}_2\text{CNRR}')_2$. Of these, 12 feature secondary Sn···S interactions which, with (I), means approximately 10% of all $R_2\text{Sn}(\text{S}_2\text{CNRR}')_2$ structures have Sn···S secondary interactions. Selected geometric details for the 13 structures are collated in Table 5. The Sn···S interactions assemble molecules in their crystals into three distinct structural motifs. The common motif, *A*, is a dimeric aggregate disposed about a centre of inversion, as is in (I), and is found in the majority of crystals, *i.e.* nine. This motif is illustrated in Fig. 7a for (PhCH₂)₂Sn(S₂CNEt₂)₂ (Yin *et al.*, 2003). A second zero-dimensional motif, *B*, is also known and is readily related to *A*. In the structure of Me₂Sn(S₂CN(Et)CH₂C₆H₄N-4)₂ (Barba *et al.*, 2012), two independent molecules comprise the asymmetric unit. One of these self-assembles about a centre of inversion as for motif *A*. The nitrogen atom of each pendent 4-pyridyl group of the dimeric aggregate thus assembled interacts with the tin atom of the second independent molecule *via* a Sn···N interaction to form the four-molecule aggregate shown in Fig. 7b. The final three molecules are binuclear owing to the presence of bis(dithiocarbamate) ligands and self-assemble into supramolecular chains. In {Me₂SnS₂CN(CH₂Ph)CH₂(1,3-C₆H₃)CH₂(PhCH₂)NCS₂SnMe₂}₂ (Santacruz-Juárez *et al.*, 2008), the molecule is situated about a centre of inversion and each tin atom forms an Sn···S contact to generate a linear, supramolecular chain, motif *C*, Fig. 7c. A

variation is seen in the crystal of Me₂SnS₂CN(CH₂CH₂-*i*-Pr)CH₂(1,3-C₆H₃)CH₂(PhCH₂)NCS₂SnMe₂}₂, where there are two independent, centrosymmetric molecules in the asymmetric unit. Here, the resulting supramolecular chain is twisted (Santacruz-Juárez *et al.*, 2008) and is assigned as motif *C'*.

The common feature of all motifs listed in Table 5 is that it is one of the weakly bound sulfur atoms that forms the

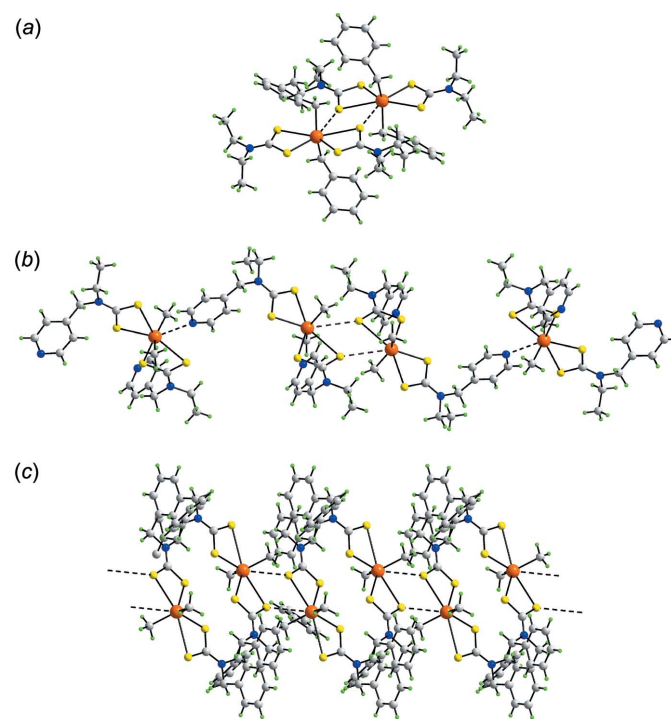


Figure 7
Supramolecular aggregation sustained by secondary Sn···S interactions (black dashed lines) leading to (a) dimeric aggregates in (PhCH₂)₂Sn(S₂CNEt₂)₂, (b) four-molecule aggregates in Me₂Sn(S₂CN(Et)CH₂C₆H₄N-4)₂ and (c) linear supramolecular chain in {Me₂SnS₂CN(CH₂Ph)CH₂(1,3-C₆H₃)CH₂(PhCH₂)NCS₂SnMe₂}₂.

secondary Sn···S interaction. Further, the tin-bound groups are relatively sterically unencumbered, allowing for the close approach of sulfur donors to the tin atoms. There are no geometric correlations. However, reflecting the weak nature of these interactions, the sulfur atom forming the Sn···S contact does not necessarily form the weaker of the Sn—S_{long} interactions in each molecule. The range of Sn···S distances spans nearly 0.5 Å but, again, no correlations between these distances and the S_{long}—Sn—S_{long} angles is apparent, *i.e.* it might be expected that the shorter Sn···S interactions would result in wider S_{long}—Sn—S_{long} angles.

6. Synthesis and crystallization

All chemicals and solvents were used as purchased without purification, and all reactions were carried out under ambient conditions. The melting point was determined using an Electrothermal digital melting point apparatus and was uncorrected. The IR spectrum for (I) was obtained on a Perkin Elmer Spectrum 400 FT Mid-IR/Far-IR spectrophotometer in the range 4000 to 400 cm⁻¹. The ¹H NMR spectrum was recorded at room temperature in CDCl₃ solution on a Jeol ECA 400 MHz FT-NMR spectrometer.

Sodium morpholinedithiocarbamate (prepared from the reaction between carbon disulfide and morpholine (Merck) in the presence of sodium hydroxide; 1.0 mmol, 0.185 g) in methanol (20 ml) was added to dimethyltin dichloride (Merck, 1.0 mmol, 0.219 g) in methanol (10 ml). The resulting mixture was stirred and refluxed for 2 h. The filtrate was evaporated until an off-white precipitate was obtained. The precipitate was recrystallized from methanol solution by slow evaporation to yield colourless prisms. Yield: 0.305 g, 64.4%; m.p.: 448 K. IR (cm⁻¹): 1465(*s*), 1423(*s*) ν(C—N), 1222(*s*) ν(C—O), 1110(*m*), 994(*s*) ν(C—S), 541(*m*) ν(Sn—C) cm⁻¹. ¹H NMR (CDCl₃): 4.18 (*s*, 8H, CH₂O), 3.77 (*s*, 8H, NCH₂), 1.54 (*s*, 6H, -CH₃).

7. Refinement

Crystal data, data collection and structure refinement details are summarized in Table 6. Carbon-bound H atoms were placed in calculated positions (C—H = 0.98–0.99 Å) and were included in the refinement in the riding-model approximation, with *U*_{iso}(H) set to 1.2–1.5*U*_{eq}(C). Owing to poor agreement, one reflection, *i.e.* ($\bar{1}2$ 1 5), was omitted from the final cycles of refinement.

Acknowledgements

The authors are grateful to Sunway University (INT-RRO-2017-096), the University of Malaya (award Nos. RP017B-14AFR and PG168-2016A) and the Ministry of Higher Education of Malaysia (MOHE) Fundamental Research Grant Scheme (grant No. FP033-2014B) for supporting this research.

Table 6
Experimental details.

Crystal data	
Chemical formula	[Sn(CH ₃) ₂ (C ₅ H ₈ NOS ₂) ₂]
<i>M</i> _r	473.24
Crystal system, space group	Monoclinic, <i>P</i> 2 ₁ / <i>n</i>
Temperature (K)	100
<i>a</i> , <i>b</i> , <i>c</i> (Å)	10.1472 (1), 13.6653 (1), 13.8122 (1)
β (°)	104.959 (1)
<i>V</i> (Å ³)	1850.36 (3)
<i>Z</i>	4
Radiation type	Cu Kα
μ (mm ⁻¹)	15.25
Crystal size (mm)	0.24 × 0.09 × 0.06
Data collection	
Diffractometer	Agilent SuperNova, Dual, Cu at zero, AtlasS2
Absorption correction	Gaussian (<i>CrysAlis PRO</i> ; Rigaku Oxford Diffraction, 2015)
<i>T</i> _{min} , <i>T</i> _{max}	0.242, 0.759
No. of measured, independent and observed [<i>I</i> > 2σ(<i>I</i>)] reflections	19588, 3865, 3809
<i>R</i> _{int}	0.031
(sin θ/λ) _{max} (Å ⁻¹)	0.631
Refinement	
<i>R</i> [<i>F</i> ² > 2σ(<i>F</i> ²)], <i>wR</i> (<i>F</i> ²), <i>S</i>	0.024, 0.065, 1.07
No. of reflections	3865
No. of parameters	192
H-atom treatment	H-atom parameters constrained
Δρ _{max} , Δρ _{min} (e Å ⁻³)	0.45, -0.50

Computer programs: *CrysAlis PRO* (Rigaku Oxford Diffraction, 2015), *SHELXS* (Sheldrick, 2008), *SHELXL2014* (Sheldrick, 2015), *ORTEP-3 for Windows* (Farrugia, 2012), *DIAMOND* (Brandenburg, 2006) and *pubCIF* (Westrip, 2010).

References

- Alcock, N. W. (1972). *Adv. Inorg. Chem. Radiochem.* **15**, 1–58.
 Barba, V., Arenaza, B., Guerrero, J. & Reyes, R. (2012). *Heteroat. Chem.* **23**, 422–428.
 Bondi, A. (1964). *J. Phys. Chem.* **68**, 441–451.
 Brandenburg, K. (2006). *DIAMOND*. Crystal Impact GbR, Bonn, Germany.
 Farrugia, L. J. (2012). *J. Appl. Cryst.* **45**, 849–854.
 Ferreira, I. P., de Lima, G. M., Paniago, E. B., Rocha, W. R., Takahashi, J. A., Pinheiro, C. B. & Ardisson, J. D. (2012). *Eur. J. Med. Chem.* **58**, 493–503.
 Ferreira, I. P., de Lima, G. M., Paniago, E. B., Rocha, W. R., Takahashi, J. A., Pinheiro, C. B. & Ardisson, J. D. (2014). *Polyhedron*, **79**, 161–169.
 Groom, C. R., Bruno, I. J., Lightfoot, M. P. & Ward, S. C. (2016). *Acta Cryst.* **B72**, 171–179.
 Hall, V. J. & Tiekink, E. R. T. (1998). *Main Group Met. Chem.* **21**, 245–254.
 Kevin, P., Lewis, D. J., Raftery, J., Malik, M. A. & O'Brien, P. (2015). *J. Cryst. Growth*, **415**, 93–99.
 Kim, K., Ibers, J. A., Jung, O.-S. & Sohn, Y. S. (1987). *Acta Cryst.* **C43**, 2317–2319.
 Marín-Luna, M., Alkorta, I. & Elguero, J. (2016). *J. Phys. Chem. A*, **120**, 648–656.
 McKinnon, J. J., Jayatilaka, D. & Spackman, M. A. (2007). *Chem. Commun.* pp. 3814–3816.
 Mohamad, R., Awang, N., Jotani, M. M. & Tiekink, E. R. T. (2016). *Acta Cryst.* **E72**, 1130–1137.
 Mohamad, R., Awang, N., Kamaludin, N. F., Jotani, M. M. & Tiekink, E. R. T. (2017). *Acta Cryst.* **E73**, 260–265.

- Morris, J. S. & Schlemper, E. O. (1979). *J. Cryst. Mol. Struct.* **9**, 13–31.
- Muthalib, A. F. A., Baba, I., Khaledi, H., Ali, H. M. & Tiekink, E. R. T. (2014). *Z. Kristallogr.* **229**, 39–46.
- Ng, S. W., Wei, C., Kumar Das, V. G., Jameson, G. B. & Butcher, R. J. (1989). *J. Organomet. Chem.* **365**, 75–82.
- Rigaku Oxford Diffraction (2015). *CrysAlis PRO*. Agilent Technologies Inc., Santa Clara, CA, USA.
- Rojas-León, I., Guerrero-Alvarez, J. A., Hernández-Paredes, J. & Höpfl, H. (2012). *Chem. Commun.* **48**, 401–403.
- Santacruz-Juárez, E., Cruz-Huerta, J., Hernández-Ahuactzi, I. F., Reyes-Martínez, R., Tlahuext, H., Morales-Rojas, H. & Höpfl, H. (2008). *Inorg. Chem.* **47**, 9804–9812.
- Sheldrick, G. M. (2008). *Acta Cryst.* **A64**, 112–122.
- Sheldrick, G. M. (2015). *Acta Cryst.* **C71**, 3–8.
- Tiekink, E. R. T. (2008). *Appl. Organomet. Chem.* **22**, 533–550.
- Tiekink, E. R. T. (2017). *Coord. Chem. Rev.* <http://dx.doi.org/10.1016/j.ccr.2017.01.009>.
- Westrip, S. P. (2010). *J. Appl. Cryst.* **43**, 920–925.
- Xue, S., Yin, H., Wang, Q. & Wang, D. (2005). *Heteroat. Chem.* **16**, 271–277.
- Yin, H. D., Wang, C.-H., Wang, Y. & Ma, C.-L. (2003). *Chin. J. Chem.* **21**, 356–360.
- Yin, H. D. & Xue, S. C. (2005a). *Appl. Organomet. Chem.* **19**, 194.
- Yin, H. D. & Xue, S. C. (2005b). *Appl. Organomet. Chem.* **19**, 187.
- Yin, H. D. & Xue, S. C. (2006). *Appl. Organomet. Chem.* **20**, 283–289.
- Yu, Y., Yang, H., Wei, Z.-W. & Tang, L.-F. (2014). *Heteroat. Chem.* **25**, 274–281.
- Zia-ur-Rehman, Shahzadi, S., Ali, S. & Jin, G.-X. (2007). *Turk. J. Chem.* **31**, 435–442.

supporting information

Acta Cryst. (2017). E73, 842-848 [https://doi.org/10.1107/S2056989017006855]

Secondary bonding in dimethylbis(morpholine-4-carbodithioato- κ^2S,S')tin(IV): crystal structure and Hirshfeld surface analysis

Nordiyana Binti Zaldi, Rusnah Syahila Duali Hussen, See Mun Lee, Nathan R. Halcovitch, Mukesh M. Jotani and Edward R. T. Tiekink

Computing details

Data collection: *CrysAlis PRO* (Rigaku Oxford Diffraction, 2015); cell refinement: *CrysAlis PRO* (Rigaku Oxford Diffraction, 2015); data reduction: *CrysAlis PRO* (Rigaku Oxford Diffraction, 2015); program(s) used to solve structure: *SHELXS* (Sheldrick, 2008); program(s) used to refine structure: *SHELXL2014* (Sheldrick, 2015); molecular graphics: *ORTEP-3 for Windows* (Farrugia, 2012) and *DIAMOND* (Brandenburg, 2006); software used to prepare material for publication: *publCIF* (Westrip, 2010).

Dimethylbis(morpholine-4-carbodithioato- κ^2S,S')tin(IV)

Crystal data

[Sn(CH₃)₂(C₅H₈NOS₂)₂]

$M_r = 473.24$

Monoclinic, $P2_1/n$

$a = 10.1472$ (1) Å

$b = 13.6653$ (1) Å

$c = 13.8122$ (1) Å

$\beta = 104.959$ (1)°

$V = 1850.36$ (3) Å³

$Z = 4$

$F(000) = 952$

$D_x = 1.699$ Mg m⁻³

Cu $K\alpha$ radiation, $\lambda = 1.54184$ Å

Cell parameters from 14936 reflections

$\theta = 3.2\text{--}76.6^\circ$

$\mu = 15.25$ mm⁻¹

$T = 100$ K

Prism, colourless

$0.24 \times 0.09 \times 0.06$ mm

Data collection

Agilent SuperNova, Dual, Cu at zero, AtlasS2 diffractometer

Radiation source: micro-focus sealed X-ray tube, SuperNova (Cu) X-ray Source

Mirror monochromator

ω scans

Absorption correction: gaussian (CrysAlis PRO; Rigaku Oxford Diffraction, 2015)

$T_{\min} = 0.242$, $T_{\max} = 0.759$

19588 measured reflections

3865 independent reflections

3809 reflections with $I > 2\sigma(I)$

$R_{\text{int}} = 0.031$

$\theta_{\max} = 76.8^\circ$, $\theta_{\min} = 4.6^\circ$

$h = -12 \rightarrow 12$

$k = -13 \rightarrow 17$

$l = -17 \rightarrow 17$

Refinement

Refinement on F^2

Least-squares matrix: full

$R[F^2 > 2\sigma(F^2)] = 0.024$

$wR(F^2) = 0.065$

$S = 1.07$

3865 reflections

192 parameters

0 restraints

Hydrogen site location: inferred from neighbouring sites

H-atom parameters constrained

$$w = 1/[\sigma^2(F_o^2) + (0.0322P)^2 + 2.5554P]$$

where $P = (F_o^2 + 2F_c^2)/3$
 $(\Delta/\sigma)_{\max} = 0.001$

$$\Delta\rho_{\max} = 0.45 \text{ e } \text{\AA}^{-3}$$

$$\Delta\rho_{\min} = -0.50 \text{ e } \text{\AA}^{-3}$$

Special details

Geometry. All esds (except the esd in the dihedral angle between two l.s. planes) are estimated using the full covariance matrix. The cell esds are taken into account individually in the estimation of esds in distances, angles and torsion angles; correlations between esds in cell parameters are only used when they are defined by crystal symmetry. An approximate (isotropic) treatment of cell esds is used for estimating esds involving l.s. planes.

Fractional atomic coordinates and isotropic or equivalent isotropic displacement parameters (\AA^2)

	<i>x</i>	<i>y</i>	<i>z</i>	$U_{\text{iso}}^*/U_{\text{eq}}$
Sn	0.54609 (2)	0.47196 (2)	0.20083 (2)	0.01811 (6)
S1	0.60114 (7)	0.47340 (5)	0.39117 (5)	0.02266 (14)
S2	0.76105 (7)	0.60660 (4)	0.29478 (4)	0.02164 (13)
S3	0.36959 (7)	0.34005 (5)	0.20926 (4)	0.02368 (13)
S4	0.38512 (7)	0.40224 (5)	0.00694 (4)	0.02491 (14)
O1	0.9722 (2)	0.62761 (17)	0.68544 (15)	0.0315 (4)
O2	-0.1073 (2)	0.28893 (17)	-0.02186 (16)	0.0334 (5)
N1	0.7980 (2)	0.59004 (16)	0.49256 (16)	0.0216 (4)
N2	0.1802 (2)	0.29886 (17)	0.04134 (16)	0.0235 (5)
C1	0.7294 (3)	0.56096 (18)	0.40120 (18)	0.0188 (5)
C2	0.8983 (3)	0.6702 (2)	0.5084 (2)	0.0245 (5)
H2A	0.8543	0.7321	0.5205	0.029*
H2B	0.9318	0.6786	0.4477	0.029*
C3	1.0169 (3)	0.6474 (2)	0.5975 (2)	0.0294 (6)
H3A	1.0670	0.5899	0.5817	0.035*
H3B	1.0805	0.7036	0.6103	0.035*
C4	0.8853 (3)	0.5444 (2)	0.6688 (2)	0.0285 (6)
H4A	0.8579	0.5290	0.7309	0.034*
H4B	0.9355	0.4874	0.6522	0.034*
C5	0.7594 (3)	0.5622 (2)	0.58459 (19)	0.0253 (5)
H5A	0.7031	0.5021	0.5722	0.030*
H5B	0.7044	0.6151	0.6037	0.030*
C6	0.2990 (3)	0.34278 (18)	0.07953 (18)	0.0202 (5)
C7	0.1020 (3)	0.2459 (2)	0.1005 (2)	0.0267 (6)
H7A	0.1494	0.2502	0.1726	0.032*
H7B	0.0943	0.1760	0.0810	0.032*
C8	-0.0379 (3)	0.2905 (2)	0.0819 (2)	0.0310 (6)
H8A	-0.0919	0.2539	0.1201	0.037*
H8B	-0.0296	0.3590	0.1061	0.037*
C9	-0.0330 (3)	0.3430 (2)	-0.0777 (2)	0.0303 (6)
H9A	-0.0261	0.4120	-0.0551	0.036*
H9B	-0.0829	0.3418	-0.1495	0.036*
C10	0.1087 (3)	0.3021 (2)	-0.06570 (19)	0.0249 (5)
H10A	0.1028	0.2354	-0.0945	0.030*
H10B	0.1599	0.3439	-0.1020	0.030*
C11	0.4147 (3)	0.5961 (2)	0.1692 (2)	0.0260 (5)

H11A	0.4573	0.6513	0.2110	0.039*
H11B	0.3275	0.5803	0.1837	0.039*
H11C	0.3987	0.6137	0.0983	0.039*
C12	0.7041 (3)	0.38945 (19)	0.1667 (2)	0.0242 (5)
H12A	0.7154	0.4095	0.1012	0.036*
H12B	0.6809	0.3197	0.1650	0.036*
H12C	0.7894	0.4008	0.2181	0.036*

Atomic displacement parameters (Å²)

	U^{11}	U^{22}	U^{33}	U^{12}	U^{13}	U^{23}
Sn	0.02190 (10)	0.01935 (10)	0.01260 (9)	0.00090 (6)	0.00357 (6)	-0.00052 (5)
S1	0.0275 (3)	0.0258 (3)	0.0140 (3)	-0.0074 (2)	0.0041 (2)	-0.0009 (2)
S2	0.0290 (3)	0.0213 (3)	0.0154 (3)	-0.0032 (2)	0.0069 (2)	-0.0006 (2)
S3	0.0290 (3)	0.0286 (3)	0.0117 (3)	-0.0060 (2)	0.0022 (2)	0.0025 (2)
S4	0.0282 (3)	0.0332 (3)	0.0131 (3)	-0.0068 (3)	0.0051 (2)	0.0014 (2)
O1	0.0294 (10)	0.0400 (11)	0.0208 (9)	-0.0022 (9)	-0.0013 (8)	-0.0006 (8)
O2	0.0246 (10)	0.0416 (12)	0.0313 (11)	-0.0046 (9)	0.0025 (8)	-0.0013 (9)
N1	0.0257 (11)	0.0236 (10)	0.0149 (10)	-0.0024 (9)	0.0041 (8)	-0.0016 (8)
N2	0.0258 (11)	0.0271 (11)	0.0163 (10)	-0.0043 (9)	0.0033 (9)	0.0012 (9)
C1	0.0234 (12)	0.0153 (11)	0.0168 (11)	0.0006 (9)	0.0036 (9)	-0.0018 (9)
C2	0.0249 (13)	0.0256 (13)	0.0201 (12)	-0.0042 (10)	0.0007 (10)	-0.0027 (10)
C3	0.0248 (13)	0.0337 (15)	0.0273 (14)	0.0014 (11)	0.0023 (11)	0.0002 (12)
C4	0.0323 (15)	0.0301 (14)	0.0208 (13)	0.0020 (12)	0.0029 (11)	0.0029 (11)
C5	0.0291 (14)	0.0320 (14)	0.0140 (11)	-0.0044 (11)	0.0040 (10)	-0.0019 (10)
C6	0.0233 (12)	0.0204 (11)	0.0160 (11)	0.0013 (9)	0.0037 (9)	-0.0002 (9)
C7	0.0293 (14)	0.0290 (13)	0.0212 (12)	-0.0091 (11)	0.0053 (11)	0.0022 (11)
C8	0.0284 (14)	0.0373 (15)	0.0278 (14)	-0.0074 (12)	0.0083 (11)	-0.0038 (12)
C9	0.0300 (14)	0.0314 (15)	0.0253 (13)	-0.0019 (12)	-0.0002 (11)	-0.0020 (11)
C10	0.0265 (13)	0.0295 (13)	0.0161 (12)	-0.0074 (11)	0.0010 (10)	-0.0027 (10)
C11	0.0279 (13)	0.0244 (13)	0.0260 (13)	0.0111 (11)	0.0074 (11)	0.0042 (10)
C12	0.0264 (13)	0.0222 (12)	0.0228 (12)	0.0052 (10)	0.0043 (10)	-0.0042 (10)

Geometric parameters (Å, °)

Sn—S1	2.5429 (6)	C3—H3A	0.9900
Sn—S2	2.8923 (6)	C3—H3B	0.9900
Sn—S3	2.5649 (7)	C4—C5	1.509 (4)
Sn—S4	2.9137 (6)	C4—H4A	0.9900
Sn—C11	2.132 (3)	C4—H4B	0.9900
Sn—C12	2.111 (3)	C5—H5A	0.9900
C1—S1	1.747 (3)	C5—H5B	0.9900
C1—S2	1.702 (3)	C7—C8	1.505 (4)
C6—S3	1.750 (3)	C7—H7A	0.9900
C6—S4	1.697 (3)	C7—H7B	0.9900
O1—C4	1.421 (4)	C8—H8A	0.9900
O1—C3	1.428 (4)	C8—H8B	0.9900
O2—C9	1.418 (4)	C9—C10	1.512 (4)

O2—C8	1.424 (4)	C9—H9A	0.9900
N1—C1	1.335 (3)	C9—H9B	0.9900
N1—C2	1.472 (3)	C10—H10A	0.9900
N1—C5	1.473 (3)	C10—H10B	0.9900
N2—C6	1.328 (4)	C11—H11A	0.9800
N2—C7	1.468 (3)	C11—H11B	0.9800
N2—C10	1.470 (3)	C11—H11C	0.9800
C2—C3	1.515 (4)	C12—H12A	0.9800
C2—H2A	0.9900	C12—H12B	0.9800
C2—H2B	0.9900	C12—H12C	0.9800
S1—Sn—S2	65.935 (19)	H4A—C4—H4B	108.0
S1—Sn—S3	85.878 (19)	N1—C5—C4	110.3 (2)
S1—Sn—S4	150.95 (2)	N1—C5—H5A	109.6
S1—Sn—C11	99.49 (8)	C4—C5—H5A	109.6
S1—Sn—C12	104.96 (8)	N1—C5—H5B	109.6
S2—Sn—S3	151.798 (18)	C4—C5—H5B	109.6
S2—Sn—S4	143.066 (18)	H5A—C5—H5B	108.1
S2—Sn—C11	86.87 (8)	N2—C6—S4	122.32 (19)
S2—Sn—C12	84.93 (8)	N2—C6—S3	119.1 (2)
S3—Sn—S4	65.137 (18)	S4—C6—S3	118.56 (15)
S3—Sn—C12	102.37 (8)	N2—C7—C8	109.1 (2)
S3—Sn—C11	99.28 (8)	N2—C7—H7A	109.9
S4—Sn—C11	84.20 (8)	C8—C7—H7A	109.9
S4—Sn—C12	84.15 (7)	N2—C7—H7B	109.9
C11—Sn—C12	148.24 (11)	C8—C7—H7B	109.9
C1—S1—Sn	92.73 (8)	H7A—C7—H7B	108.3
C1—S2—Sn	82.29 (9)	O2—C8—C7	111.4 (2)
C6—S3—Sn	92.55 (9)	O2—C8—H8A	109.3
C6—S4—Sn	82.27 (9)	C7—C8—H8A	109.3
C4—O1—C3	109.5 (2)	O2—C8—H8B	109.3
C9—O2—C8	110.2 (2)	C7—C8—H8B	109.3
C1—N1—C2	122.2 (2)	H8A—C8—H8B	108.0
C1—N1—C5	123.3 (2)	O2—C9—C10	111.8 (2)
C2—N1—C5	113.0 (2)	O2—C9—H9A	109.2
C6—N2—C7	124.6 (2)	C10—C9—H9A	109.2
C6—N2—C10	123.2 (2)	O2—C9—H9B	109.2
C7—N2—C10	112.2 (2)	C10—C9—H9B	109.2
N1—C1—S2	122.6 (2)	H9A—C9—H9B	107.9
N1—C1—S1	118.35 (19)	N2—C10—C9	109.3 (2)
S2—C1—S1	119.04 (14)	N2—C10—H10A	109.8
N1—C2—C3	110.0 (2)	C9—C10—H10A	109.8
N1—C2—H2A	109.7	N2—C10—H10B	109.8
C3—C2—H2A	109.7	C9—C10—H10B	109.8
N1—C2—H2B	109.7	H10A—C10—H10B	108.3
C3—C2—H2B	109.7	Sn—C11—H11A	109.5
H2A—C2—H2B	108.2	Sn—C11—H11B	109.5
O1—C3—C2	111.7 (2)	H11A—C11—H11B	109.5

O1—C3—H3A	109.3	Sn—C11—H11C	109.5
C2—C3—H3A	109.3	H11A—C11—H11C	109.5
O1—C3—H3B	109.3	H11B—C11—H11C	109.5
C2—C3—H3B	109.3	Sn—C12—H12A	109.5
H3A—C3—H3B	107.9	Sn—C12—H12B	109.5
O1—C4—C5	111.3 (2)	H12A—C12—H12B	109.5
O1—C4—H4A	109.4	Sn—C12—H12C	109.5
C5—C4—H4A	109.4	H12A—C12—H12C	109.5
O1—C4—H4B	109.4	H12B—C12—H12C	109.5
C5—C4—H4B	109.4		
C2—N1—C1—S2	5.5 (4)	C7—N2—C6—S4	179.6 (2)
C5—N1—C1—S2	171.0 (2)	C10—N2—C6—S4	-3.5 (4)
C2—N1—C1—S1	-173.9 (2)	C7—N2—C6—S3	-0.7 (4)
C5—N1—C1—S1	-8.4 (3)	C10—N2—C6—S3	176.2 (2)
Sn—S2—C1—N1	179.7 (2)	Sn—S4—C6—N2	168.6 (2)
Sn—S2—C1—S1	-0.98 (13)	Sn—S4—C6—S3	-11.13 (13)
Sn—S1—C1—N1	-179.5 (2)	Sn—S3—C6—N2	-167.2 (2)
Sn—S1—C1—S2	1.11 (15)	Sn—S3—C6—S4	12.56 (15)
C1—N1—C2—C3	-143.1 (3)	C6—N2—C7—C8	122.6 (3)
C5—N1—C2—C3	50.1 (3)	C10—N2—C7—C8	-54.6 (3)
C4—O1—C3—C2	61.3 (3)	C9—O2—C8—C7	-60.3 (3)
N1—C2—C3—O1	-55.1 (3)	N2—C7—C8—O2	57.4 (3)
C3—O1—C4—C5	-61.7 (3)	C8—O2—C9—C10	59.5 (3)
C1—N1—C5—C4	142.5 (3)	C6—N2—C10—C9	-123.5 (3)
C2—N1—C5—C4	-50.8 (3)	C7—N2—C10—C9	53.7 (3)
O1—C4—C5—N1	56.3 (3)	O2—C9—C10—N2	-55.8 (3)

Hydrogen-bond geometry (Å, °)

Cg1 is the centroid of the (C8–C13) ring.

<i>D</i> —H... <i>A</i>	<i>D</i> —H	H... <i>A</i>	<i>D</i> ... <i>A</i>	<i>D</i> —H... <i>A</i>
C10—H10 <i>A</i> ...S1 ⁱ	0.99	2.86	3.809 (3)	161
C12—H12 <i>C</i> ...O1 ⁱⁱ	0.98	2.47	3.399 (4)	158

Symmetry codes: (i) $x-3/2, -y-1/2, z-3/2$; (ii) $-x+2, -y+1, -z+1$.